



Research Article

Effects of Sheep Bone Peptide-Chelated Calcium on Calcium Absorption and Bone Deposition in Rats Fed a Low-Calcium Diet

Guanhua Hu,^{1,2} Xiaotong Li,^{1,2} Rina Su,³ Mirco Corazzin,⁴ Lu Dou,^{1,2} Lina Sun,^{1,2} Puxin Hou,⁵ Lin Su,^{1,2} Ye Jin ,^{1,2} and Lihua Zhao ^{1,2}

¹College of Food Science and Engineering, Inner Mongolia Agricultural University, Hohhot 010018, China

²Integrative Research Base of Beef and Lamb Processing Technology,

Ministry of Agriculture and Rural Affairs of the People's Republic of China, Hohhot 010018, China

³Inner Mongolia Vocational College of Chemical Engineering, Hohhot 010010, China

⁴Department of Agricultural, Food, Environmental and Animal Sciences, University of Udine, Udine 33100, Italy

⁵Science and Technology Achievement Transformation Center, Bayan Nur 015000, China

Correspondence should be addressed to Ye Jin; jinyeyc@sohu.com and Lihua Zhao; zhaolihua@imau.edu.cn

Received 11 January 2024; Revised 8 March 2024; Accepted 12 March 2024; Published 3 April 2024

Academic Editor: Mohamed Afifi

Copyright © 2024 Guanhua Hu et al. This is an open access article distributed under the Creative Commons Attribution License, which permits unrestricted use, distribution, and reproduction in any medium, provided the original work is properly cited.

Sheep bones, as the main byproduct after sheep slaughter, are rich in proteins, but their utilization in deep processing is relatively low. Currently, calcium deficiency is a common health issue that can lead to metabolic bone diseases. Peptide calcium chelate is considered a superior substance, having a significant effect on improving the absorption and utilization efficiency of calcium in the human body. This study used sheep bone byproducts as the raw material to prepare sheep bone peptide-chelated calcium (SBP-Ca) and its structure was characterized and analyzed in depth. SBP-Ca was supplemented in a low-calcium diet to assess its effects on calcium absorption and bone formation in a rat model experiencing calcium deficiency. The results showed that under optimal preparation conditions for SBP-Ca (peptide-calcium ratio set at 1 : 1, pH maintained at 7, temperature set to 45°C, and duration of 60 min), calcium could chelate with sheep bone peptide (SBP) at the sites C=O, -NH₂, and -COOH sites, forming a structurally dense SBP-Ca with a chelation rate of up to 89.24%. In rats fed a low-calcium diet, SBP-Ca significantly improved the rat femoral diameter, dry weight, trabecular bone structure, bone density, and bone volume fraction ($P < 0.05$). A decline in serum alkaline phosphatase levels ($P < 0.05$), elevation in bone calcium content, and a rise in serum osteocalcin levels ($P < 0.05$) were observed. Furthermore, morphological studies on bone tissue suggest that SBP-Ca has the ability to restore trabecular bone structure. In conclusion, SBP-Ca has been successfully prepared as a novel calcium absorption promoter. By improving the bioavailability of calcium, bone formation was facilitated, demonstrating a significant application value in the prevention of calcium deficiency disorders.

1. Introduction

Calcium comprises 1.5–2% of the human body weight, as the predominant mineral element within the human body [1]. Calcium serves as a messenger to regulate cell division and apoptosis, was involved in maintaining capillary and cell membrane permeability, and is essential for the formation of bone and teeth. It also actively participates to diverse physiological activities including nerve conduction, cell proliferation, immune regulation, and muscle contraction.

Despite the presence of elemental calcium in foods (such as dairy products, vegetables, starchy foods, and dried fruits), dietary intake often falls short of meeting the recommended calcium requirements attributed to factors such as lactose intolerance and personal dietary preferences [2, 3]. Although the reference values in the diet range from 1.0 to 1.3 g, the average global calcium intake in humans is less than 0.6 g per day [4, 5]. Numerous studies have confirmed that inadequate calcium intake is linked to an elevated risk of osteoporosis, rickets, and other bone metabolic diseases and

even induces kidney stones and colon cancer [6]. To prevent and treat calcium deficiency and mitigate the adverse effects of inadequate calcium intake, more and more calcium supplements are entering the market, including inorganic calcium, calcium gluconate, and amino acid calcium. However, a majority of them exhibit low calcium ion concentration or limited bioavailability [7]. Over the past few years, some bioactive peptides extracted from diverse proteins sources, such as whey protein [8], tilapia skin and scale [9], pacific cod skin [10], and soybean [11, 12], can chelate with calcium ions that form peptide calcium chelates that are stable in the gastrointestinal tract and can prevent calcium precipitation in the body and effectively increase calcium absorption. In a previous study, porcine collagen peptide calcium chelate was formulated, and the calcium chelation rate was 78.38%. The outcomes from the Caco-2 cell monolayer model indicated a substantial enhancement in calcium ion transport by the complexes, mitigating the adverse impacts of phosphate and phytate [1, 13]. Wang et al. [14] prepared bovine bone collagen peptide calcium chelate and found that it was stable during heat treatment and gastrointestinal digestion, suggesting that it holds the potential function of enhancing calcium bioavailability. A large number of studies confirmed that calcium-chelated peptides can improve calcium absorption bioavailability and bone biomechanics in mice [15–18].

China's animal husbandry is very developed and is the world's most promising and fastest-growing meat market. As the main byproduct of sheep slaughter and processing, sheep bones represent about 10–20% of sheep carcasses. The collagen peptide produced after collagen hydrolysis is a kind of biologically active peptide that can protect the gastric mucosa [19], prevent and treat ulcers [20], promote sebum metabolism [21], reduce blood pressure [22], promote bone formation [23], improve bone density, prevent and treat osteoporosis [24], and other effects. Referring to previous research reports [25–27], we found that animal bones, as byproducts after slaughter, are typically discarded as waste, with only a small amount used for commercial purposes, primarily for the preparation of boiled soup, gelatin, and lower-value fertilizers. Therefore, the use of sheep bone to produce high-value-added products is an emerging challenge. Wang et al. [14] obtained peptide calcium chelate from sheep bones and it remained stable in different temperature ranges and during simulated gastrointestinal digestion. Furthermore, the good calcium-binding capabilities of the enzymatic breakdown products of sheep bone were demonstrated in a previous paper by our research group [28]. However, its effectiveness in facilitating calcium uptake and deposition in bone in living organisms remains unexplored.

The objective of this investigation was to generate peptide calcium chelate from sheep bone by stepwise enzymatic hydrolysis of alkaline protease and flavor protease, refine the optimal preparation parameters for SBP-Ca, elucidate the chelation ions' chelation sites with SBP, determine the calcium chelating ability of SBP-Ca, and characterize its properties and bioactivity. This study suggests that SBP-Ca can be used as a functional calcium-fortified food to improve calcium absorption.

2. Materials and Methods

2.1. Materials and Reagents. Fresh sheep bones were sourced from Inner Mongolia Meiyangyang Food Co., LTD. (Inner Mongolia, China). Sprague–Dawley rats (SD) (3–4 weeks) were acquired through procurement from Beijing Spyford Biotechnology Co., Ltd. (Beijing, China). Alkaline protease (200, 000 U/g-1, CAS: 9014-01-1) and flavor protease (30, 000 U/g-1, CAS: 9001-92-7) were acquired through procurement from Beijing Soleibao Technology Co., Ltd. (Beijing, China). Serum calcium (S-Ca), serum phosphorus (S-P), serum alkaline phosphatase (ALP), and osteocalcin (OCN) were all from Wuhan Xinqidi Biotechnology Co., Ltd. (Wuhan, China). Isoflurane (CAS: 26675-46-7) was acquired through procurement from Sigma-Aldrich Chemical Co., St. Louise (MO., USA). CaCl_2 (CAS: 10035-04-8), KBr (CAS: 10035-04-8), HNO_3 (CAS: 7697-37-2), and perchloric acid (CAS: 7601-90-3) were all sourced from Sinopharm Chemical Reagents Co., Ltd. (Shanghai, China).

2.2. Preparation of Defatted Sheep Bone Meal. After manually removing nonbone residues, such as meat, sheep bones were rinsed and pressure cooked at 121°C for 40 min, followed by multiple hot water washes and then subjected to drying at 80°C for 12 h. Subsequently, the sheep bones were crushed and sieved through an 80-mesh sieve to produce powder, which was soaked in anhydrous ethanol and agitated at room temperature for 24 h (change the solution once); the ratio of the sample to the solution was 1:10 (w/v). After washing with distilled water, the mixture was subjected to centrifugation at 8000 r/min for 15 min at 4°C. The precipitate was placed in a drying oven and subjected to drying at 70°C for 6 h to acquire defatted sheep bone powder, which was stored at –20°C.

2.3. Preparation of Sheep Bone Peptide (SBP). According to previous studies [29], defatted sheep bone meal was prepared as a 6% solution (w/v) in deionized water and then hydrolyzed with alkaline protease (50°C, 2 h, and pH 9) followed by flavor protease (50°C, 2 h, and pH 7.5). Following this, the substrate underwent heating at 100°C for 15 min to deactivate the enzyme, cooled to ambient temperature, and then centrifuged at 8000 r/min for 15 min at 4°C. The resulting supernatant was collected and further processed through vacuum freeze-dried to obtain SBP powder.

2.4. Preparation of Sheep Bone Peptide-Chelated Calcium (SBP-Ca). The freeze-dried SBP (10 mg/ml) was reconstituted in deionized water to a total volume of 20 mL. Add CaCl_2 to achieve SBP: CaCl_2 ratios of (0.5:1, 1:1, 2:1, 3:1, 4:1, 5:1), adjust the solution pH to 8, and react at 50°C for 50 min to determine the optimal SBP: CaCl_2 ratio. Subsequently, at a SBP: CaCl_2 ratio of 1:1, vary the solution pH (5, 6, 7, 8, 9, and 10), react at 50°C for 50 min to determine the optimal pH; with a SBP: CaCl_2 ratio of 1:1,

solution pH 7, perform water bath treatments at various temperature (40, 45, 50, 55, and 60°C) for 50 min to determine the optimal chelation temperature; and with a SBP:CaCl₂ ratio of 1:1, solution pH 7, react at 45°C for varying durations (30, 40, 50, 60, and 70 min) to determine the optimal reaction time. After the chelation reaction, absolute ethanol (8 times the volume of the reaction mixture) was then introduced into the reactant solutions for the removal of unreacted free calcium ions and SBP. The mixtures obtained were subjected to centrifugation at 8000 r/min for

15 min at 4°C. The precipitate was freeze-dried and designated as SBP-Ca. The supernatant and reactant solution were digested using a mixture of acids (HNO₃: perchloric acid, 4:1, v/v) and adjusted to a fixed volume using lanthanum solution (20 g/L). The calcium content in both the solution and the supernatant was analyzed using a flame atomic absorption spectrophotometer (ZEEnit 700P, Germany). The calculation method for the calcium chelation rate is outlined in the following:

$$\text{Calcium chelation rate (\%)} = \frac{\text{Total calcium content} - \text{Calcium content in the supernatant}}{\text{Total calcium content}} \times 100. \quad (1)$$

2.5. Structural Characterization Analysis of SBP and SBP-Ca

2.5.1. Fourier Transform Infrared (FTIR) Spectroscopy Analysis. FTIR analysis was used to examine the structural changes between SBP and SBP-Ca. SBP and SBP-Ca were thoroughly ground with dry KBr, mixed, and loaded onto the FTIR instrument (Nicolet iS20, Nicolet, USA). The spectra were quantified in the spectral range of 4000–400 cm⁻¹ with 32 scans in which the spectra were obtained at a resolution of 4 cm⁻¹ and this background spectrum was recorded by the transparent fraction of KBr [9].

2.5.2. Ultraviolet-Visible Absorption Spectroscopy (UV). The method outlined by Wu et al. [13] with some modifications. In particular, SBP and SBP-Ca were configured as a 1 mg/mL solution. The spectra were obtained using a UV spectrophotometer (TU-1810, Beijing Pu-Analysis General Instrument Co., Ltd.) within the wavelength region of 190–400 nm. The UV-vis spectrophotometer was blank calibrated using deionized water before measuring samples.

2.5.3. Differential Scanning Calorimeter (DSC) Analysis. The thermal transition characteristics of SBP and SBP-Ca were determined using a differential scanning calorimeter (JSM-7800F, Nippon Electronics Co., Ltd.) with certain adjustments to the method described by Wang et al. [14]. Among them, SBP and SBP-Ca were weighed about 3.0 mg and sealed in an aluminum crucible. Utilizing an empty aluminum crucible as a reference, scanning was performed at a temperature increase rate of 10°C/min within the temperature range of 25–200°C.

2.5.4. Scanning Electron Microscopy (SEM). The microstructure features of both SBP and SBP-Ca were analyzed using scanning electron microscopy (S-3400N, Hitachi, Japan). An appropriate amount of SBP and SBP-Ca powder samples were evenly attached to the specimen holder and coated with gold-plated film. The microscopic images were captured at a working distance ranging from 12.7 to 12.8 mm and an accelerating voltage of 25 kV.

2.6. Animal Experiment

2.6.1. Animal and Diet. The experimental animals were carried out following the Welfare and Ethics Committee and the Science and Technology Department of Inner Mongolia Agriculture University (NND2021072). Twenty-four SD male rats were kept in a controlled environment, maintaining constant temperature, humidity, and light conditions (22 ± 2°C, 60 ± 5% relative humidity, and 12 h light/dark cycle). During a preliminary experimental period of one week, the animals were fed AIN-93 diet [30]. Rats were randomly allocated into 4 groups (normal group Z; low-calcium model group D; CaCl₂ group C; SBP-Ca group T, 6 rats in each group). Group Z was fed standard AIN-93 animal feed (calcium content: 0.5%) for the entire 4-week duration of the experiment, while the other groups received the same amount of low-calcium AIN-93 diet (calcium content: 0.1%). The low-calcium diet formula was slightly modified according to the standard of the AIN-93 feed formulation and was produced by Sino Biotechnology Co., Ltd. (Hunan, China). The formula was (in mass fraction): casein 20.00%, cystine 0.30%, corn starch 39.70%, maltodextrin 13.20%, sucrose 10.00%, cellulose 5.00%, soybean oil 7.00%, multimineral M1003 3.50%, multidimensional V1001 1.00%, and tartaric acid choline 0.25%. Starting from the second week until the end of the experiment, the target calcium intake from calcium sources (CaCl₂ and SBP-Ca) was established at five times the recommended daily intake for humans calculated based on the recommended daily calcium intake of 800 mg Ca/60 kg body weight. This corresponded to a calcium intake of 13.33 × 5 mg Ca/(day·kg bw). Calcium sources were solubilized in distilled water and administered individually from the feed using the gavage feeding method.

2.6.2. Sample Collection. After the experimental period, all rats were subjected to a 12-hour fasting period, and their body length and weight were measured. Subsequently, the weight growth rate and body length growth rate were calculated. The rats were anesthetized using isoflurane, blood samples were then obtained from the eyeball, and the blood collected was centrifuged for serum separation. Rats were

sacrificed via cervical dislocation, followed by removal of the heart, liver, spleen, kidneys, and lungs, rinsed with cold 0.9% saline, wiped with filter paper, and weighed to calculate the visceral index [31]. The right and left femur and tibia were

dissected, and the surrounding soft tissues were cleaned and enveloped in saline-soaked gauze before being stored at -20°C for subsequent studies.

$$\begin{aligned} \text{Weight growth rate (\%)} &= \left(\frac{\text{Final weight} - \text{Initial weight}}{\text{Initial weight}} \right) * 100, \\ \text{Body length growth rate (\%)} &= \left(\frac{\text{Final length} - \text{Initial length}}{\text{Initial length}} \right) * 100, \\ \text{Relative organ weight} \left(\frac{\text{mg}}{\text{g}} \right) &= \frac{\text{Organ weights (mg)}}{\text{Body weight (g)}}. \end{aligned} \quad (2)$$

2.6.3. Measurement of Serum Indicators. Serum calcium (S-Ca) and serum phosphate (S-P) were determined using an automatic biochemical analyzer (Hitachi 3100, Japan). Alkaline phosphatase (ALP) and osteocalcin (OCN) were determined using commercial kits.

2.6.4. Bone Mass Assessment. The length and diameter of the central long axis of the femur bones of the rats were measured. Broken femur bones were introduced into a drying oven until the weight remained constant and weighed to calculate the dry weight (DW) of the backbone. The formula for the backbone weight index is as follows [32]:

$$\text{Bone dry weight (DW)} = \frac{\text{Dry weight}}{\text{Body weight}} \quad (3)$$

After drying, the femurs underwent carbonization in an electric furnace and were ashed at 800°C for 2 h in a muffle. The quantification of the bone calcium content was carried out using flame atomic absorption spectrometry (ZEE nit 700P, Germany).

2.6.5. Microcomputed Tomography (Micro-CT). The left femur of the rat was immersed and fixed in a 4% paraformaldehyde solution for 24–48 h, removed and rinsed three times with PBS (buffer), and stored in a 75% alcohol solution at 4°C . Then, it was scanned and analyzed using a Micro-CT (SkyScan 1176, Bruker, Germany) scanning imaging system, and 171–200 layers ($18 \mu\text{m}$ pixel size) of the femur were scanned from the fusion of the bone tissue growth plate [3]. 3D images were obtained by 3D reconstruction using CTVOX software and the scanning parameters were analyzed using CTAn software. The main indices included bone mineral density (BMD), bone volume fraction (BV/TV), trabecular thickness (Tb.Th), trabecular number (Tb.N), and trabecular spacing (Tb.Sp).

2.6.6. Hematoxylin and Eosin (H&E) Stained. Following the Micro-CT measurement, the left femur underwent fixation in methanol for decalcification. Subsequently, it was embedded and stained to facilitate morphological analysis. Both

transverse and longitudinal sections of the femur were stained with hematoxylin and eosin [32] and then the bone morphology was examined using an optical electron microscope (DM3000, Leica Instruments, Germany).

2.7. Statistical Analysis. Data analysis was performed utilizing SPSS 19.0 (SPSS Inc., Chicago, IL, USA) and Origin software (Origin Lab, Northampton, MA, USA). The normality of the data distribution was examined through the Shapiro–Wilk test. Differences between experimental groups and between process conditions were performed by one-way ANOVA. Data were considered significantly different at the level of $P < 0.05$.

3. Results and Discussion

3.1. Effect of Different Process Conditions on the Calcium-Chelating Capacity of SBP-Ca. As the chelation temperature increased from 40°C to 45°C , the calcium chelation rate increased significantly from 80.15% to 84.86% ($P < 0.05$), reaching the maximum value (Figure 1(a)). The moderate increase in temperature favors molecular movement increases the chance of molecular collision and enhances the probability of binding between calcium ions and amino acid residues, increasing the calcium chelation rate. However, the chelation reactions themselves are exothermic [33]. Therefore, since the temperature exceeded 45°C , the structures of the peptides and their complexes with calcium can be easily disrupted [34], leading to partial or complete changes in the molecular structure of SBP. Aggregation between molecules occurs, resulting in a reduction in available chelating groups for calcium ions, thus causing a decrease in the chelation efficiency. An analogous trend was noticed by Wu et al. [13], when investigating pig bone collagen peptide with calcium chelation, where the calcium-binding capacity peaked at 50°C , followed by a decrease with a further increase in temperature.

The impact of chelation time on the rate of calcium chelation is depicted in Figure 1(b). As the chelation time extended from 30 to 60 min, the chelation rate of calcium rapidly increased from 74.80% to 85.13% ($P < 0.05$), reaching

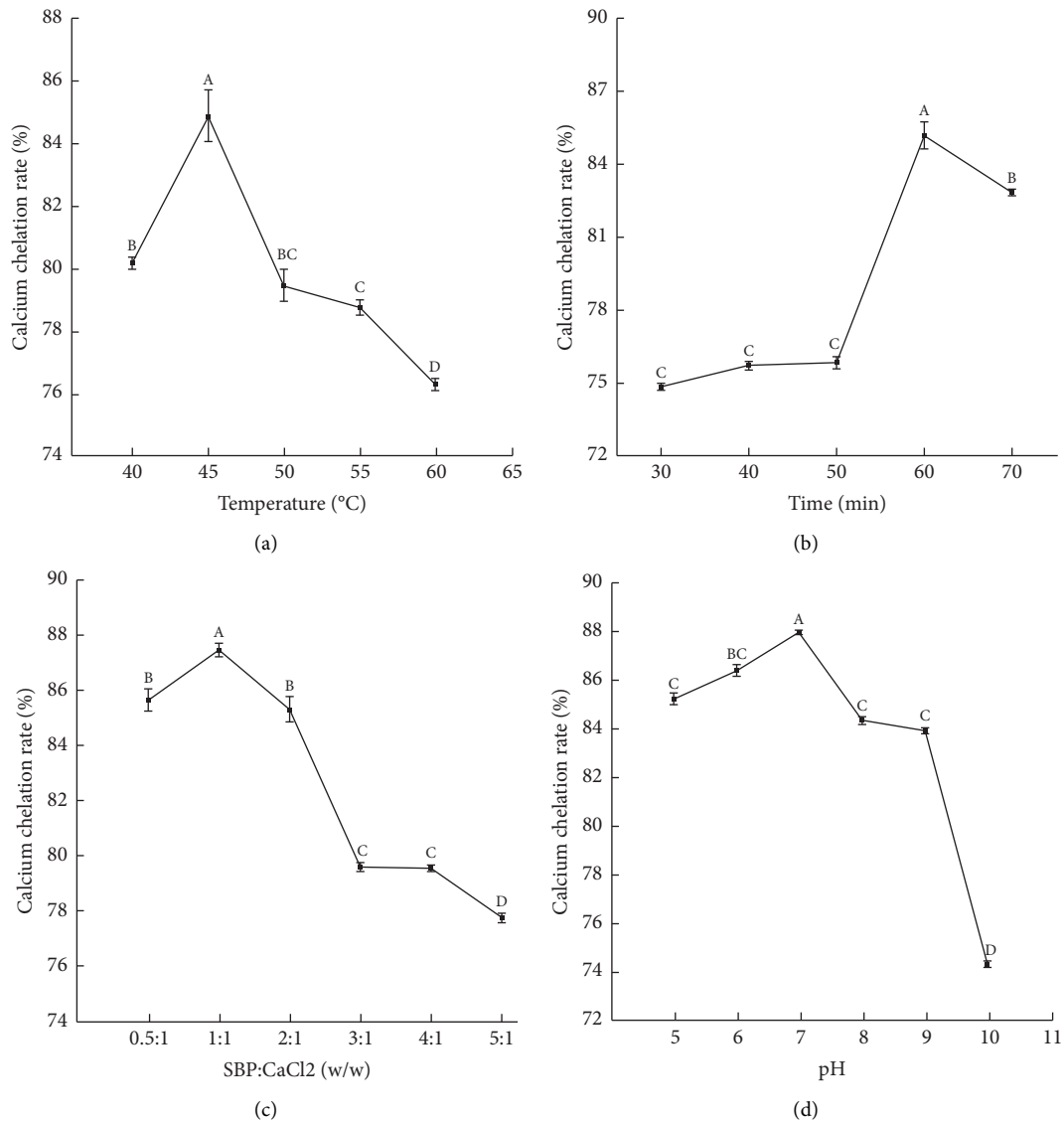


FIGURE 1: Effects of different process conditions on the calcium chelating rate of sheep bone peptide chelated calcium (SBP-Ca): (a) temperature, (b) time, (c) mass ratio of SBP/CaCl₂, and (d) pH. Data are expressed as the mean \pm sd. Different letters indicate a significant difference ($P < 0.05$).

its maximum value. However, a further extension of the reaction time resulted in a decrease in the chelation rate to 82.77% ($P < 0.05$). Also, Zhai et al. [35], in the preparation of mung bean peptide-calcium chelates, also found that the rate of calcium chelation showed a tendency to increase and then stabilize as the chelation time increased and reached a maximum at 60 min. Probably, as suggested by Fang et al. [36], with an increase in the reaction time, the contact between calcium ions and peptides increases, leading to better efficiency of the chelation reaction. However, once a certain time threshold is reached, the chelate becomes stable and the calcium chelation rate ceases to increase. Xun et al. [37] concluded that a long reaction time may lead to chelate instability and decomposition, thus reducing the chelation rate. As the mass ratio of SBP/CaCl₂ was escalated from 0.5:1 to 1:1, the chelation rate increased significantly

from 85.69% to 87.50%, reaching the maximum value ($P < 0.05$; Figure 1(c)). This phenomenon could be attributed to the increasing content of peptides in the reaction system as the SBP/CaCl₂ mass ratio increases, facilitating greater contact between calcium ions and the peptide ligand, thereby promoting the reaction in the forward direction and increasing the chelation rate. However, when the SBP/CaCl₂ mass ratio exceeded 1:1, saturation of calcium binding to peptides occurred, hindering a further improvement of the chelation rate. Similar variations in the chelation rate with the peptide-to-calcium mass ratio were observed by Cui et al. [38] in the preparation of calcium complexes with sea cucumber egg hydrolysates.

The calcium chelation rate increased from pH 5 to 7 ($P < 0.05$), reaching a maximum value of 87.96% and then decreased (Figure 1(d)). In acidic environments, a rise in

pH leads to a decline in H^+ concentration, increasing the electron-donating capacity of potential metal ion chelation sites ($-COOH$ and $-NH_2$). In alkaline environments, high concentrations of OH^- tend to form $Ca(OH)_2$ precipitates with calcium ions, resulting in a reduction in the calcium-binding capacity of SBP. Therefore, a neutral environment is the best condition for SBP to bind calcium ions, aligning with the observations of Luo et al. [39]. In conclusion, the optimal chelation process (pH = 7, temperature = $45^\circ C$, SBP/ $CaCl_2$ mass ratio = 1 : 1, and time = 60 min) was selected for the preparation of SBP-Ca, with a chelation rate as high as 89.24%, and used for subsequent analysis and animal experiments.

3.2. FTIR Analysis. As a powerful tool for studying peptide structure [40], FTIR technology has been used to further study the potential mechanism of the peptide-calcium reaction. As illustrated in Figure 2, after the addition of calcium ions, the FTIR spectrum of the SBP changed significantly; this may be caused by the change in the vibrational frequency of the amino acid moiety [41]. SBP exhibits a characteristic absorption peak at 1398.72 cm^{-1} , and a stretching change occurs in the SBP-Ca, moving to 1415.52 cm^{-1} , corresponding to the characteristic absorption region of carboxylate, indicating that the $-COOH$ in SBP chelated with calcium ions.

Simultaneously, the absorption peak of $C=O$ in SBP increased from 2943.14 cm^{-1} to 2957.13 cm^{-1} , which indicated that the carbonyl of the amide (peptide bond) contributes to the establishment of the peptide calcium chelates. This result is similar to that observed with calcium-chelated sheep bone collagen peptide obtained by the enzymatic-fermentation method [42]. Furthermore, the absorption peak corresponding to the $-NH_2$ telescopic vibration moves from 1130.78 cm^{-1} to 1146.30 cm^{-1} and the wave bandwidth becomes wider. In summary, it could be speculated that the main affinity sites of SBP encompass carboxyl oxygen, amino nitrogen, and oxygen within the peptide bond. These functional groups chelate with calcium ions to form a novel compound SBP-Ca.

3.3. Ultraviolet-Visible Absorption Spectroscopy (UV) Analysis. Ultraviolet spectroscopy is an analytical method employed to examine alterations in substances and ascertain the emergence of novel compounds [43]. Interactions between metal ions and organic ligands may result in the appearance of new absorption peaks or the shift or disappearance of the initial absorption peaks [38]. The absorption peaks of SBP and SBP-Ca were observed at 296 nm and 308 nm, respectively, as shown in Figure 3. This suggests that the conjugation effect occurs involving the π electron of carbonyl double bonds and the electrons in the lone pair on groups such as $-NH_2$ and $-OH$ when binding with calcium ions. This alteration affected the internal electron transitions of the ligand and the valence electron transitions of the corresponding atomic, resulting in a decrease in the transition energy of $n \rightarrow \sigma^*$ [44, 45]. Consequently, chelation

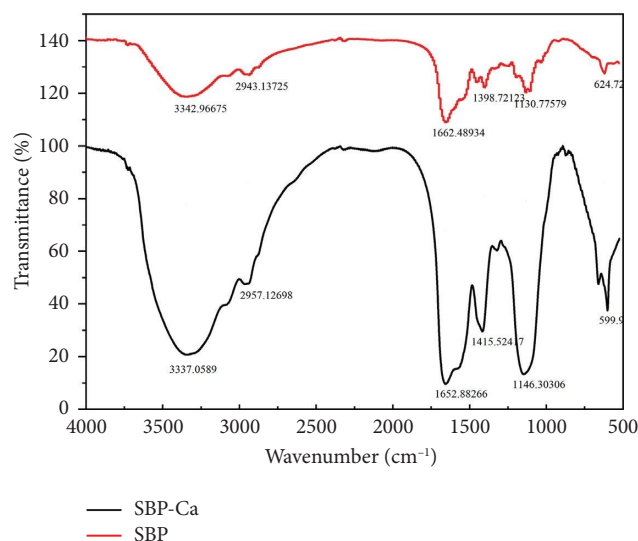


FIGURE 2: Infrared spectroscopy of sheep bone peptide (SBP) and sheep bone peptide-chelated calcium (SBP-Ca).

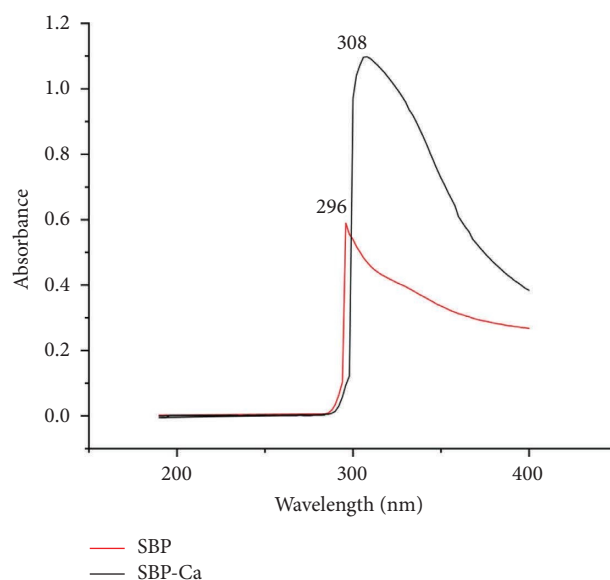


FIGURE 3: Ultraviolet scan of sheep bone peptide (SBP) and sheep bone peptide-chelated calcium (SBP-Ca).

resulted in an enhancement of absorption intensity and a redshift in the UV spectrum. Hence, it could be concluded that a new substance is formed through the chelation of peptides with calcium.

3.4. Differential Scanning Calorimetry Analysis. The SBP showed a peak of heat absorption at $172^\circ C$, which is mainly due to the breakage of chemical bonds in the SBP (Figure 4). When the SBP was chelated with calcium ions, the peak of heat absorption occurred at $155^\circ C$. The difference between the two heat absorption peaks may be ascribed to the different positions of the $C-N$ bond and the different energy and temperature required to break the $C-N$ bond at elevated temperatures [42].

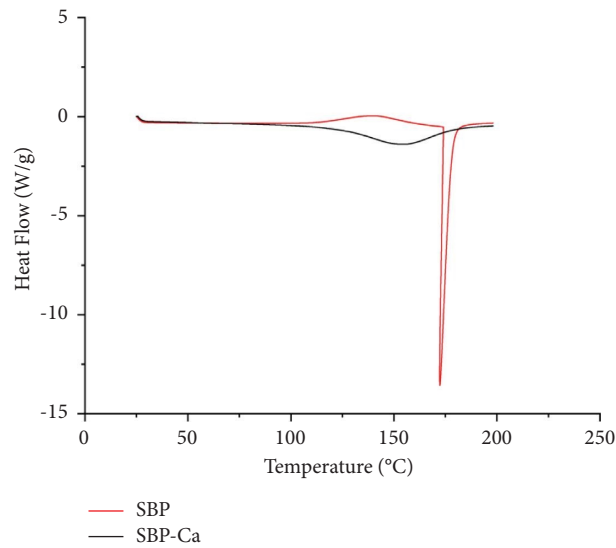


FIGURE 4: Differential scanning calorimetry (DSC) diagrams of sheep bone peptide (SBP) and sheep bone peptide-chelated calcium (SBP-Ca).

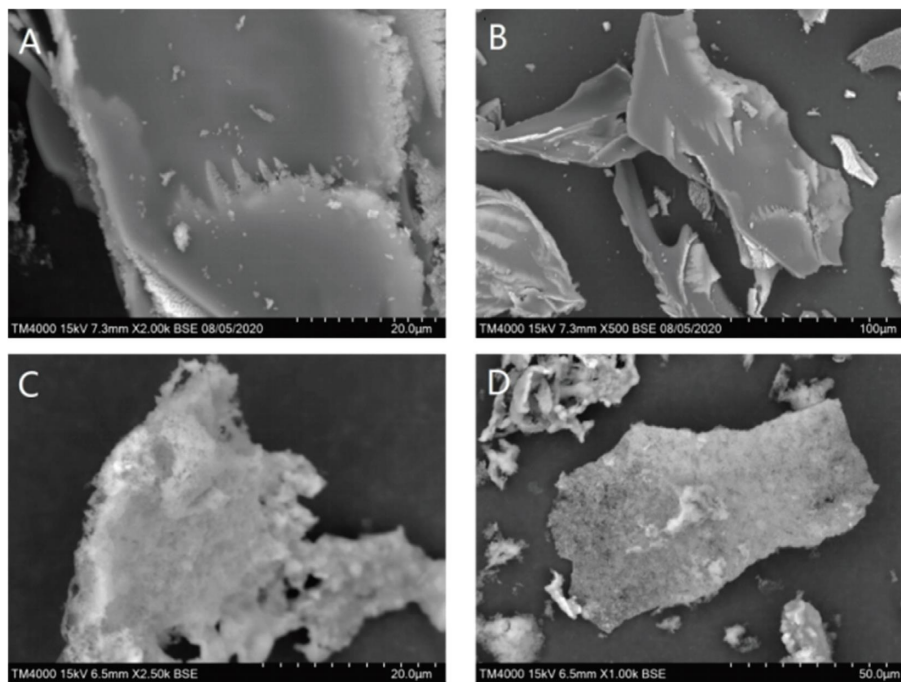


FIGURE 5: Scanning electron microscope images of sheep bone peptide (SBP) (A-B) and sheep bone peptide-chelated calcium (SBP-Ca) (C-D).

3.5. Analysis of SEM. The microstructures of SBP and SBP-Ca are displayed in Figure 5; the surface of SBP is smooth, the tissue state is delicate, and the sheet structure is present. On the contrary, the surface of SBP-Ca is rough and loose and exhibits numerous spherical formations. The variations in microstructure between SBP and SBP-Ca are probably due to the change in internal structure induced by the coordination bond formed between peptide and calcium [46].

3.6. Growth Status and Calcium Absorption in Rats. Throughout the experiment, the rats in group D exhibited reduced food intake and hair loss after 2 weeks. Rats in the other groups were flexible, had regular food intake, and exhibited normal coat color. There was no death or diarrhea in rats during the experiment. The weight growth rate of group D exhibited a marked reduction compared to the other groups ($P < 0.05$; Table 1). No significant differences were observed in body length and body length growth rate

TABLE 1: Rat body weight, body length, rate of body weight gain, and rate of body length growth.

| Groups | Rat final body weight (g) | Weight growth rate (%) | Rat final body length (cm) | Growth rate of body length (%) |
|-----------------------|---------------------------|----------------------------|----------------------------|--------------------------------|
| Control (Z) | 319.93 ± 9.85 | 143.56 ± 9.02 ^a | 17.67 ± 3.21 | 73.53 ± 1.01 |
| Low calcium (D) | 302.57 ± 14.72 | 140.02 ± 5.11 ^b | 16.99 ± 0.78 | 72.66 ± 2.05 |
| CaCl ₂ (C) | 328.68 ± 5.66 | 152.77 ± 6.80 ^a | 17.77 ± 1.22 | 73.69 ± 0.89 |
| SBP-Ca (T) | 338.63 ± 11.38 | 156.48 ± 3.03 ^a | 18.02 ± 0.32 | 73.81 ± 2.12 |

Z: rats fed with AIN-93 diet; D: rats fed with a low calcium AIN-93 diet; C: rats fed with a low calcium AIN-93 diet and CaCl₂; T: rats fed with a low calcium AIN-93 diet and SBP-Ca. The values in columns with different superscript letters are significantly different ($P < 0.05$).

TABLE 2: Organ indices of rat heart, liver, spleen, kidneys, and lungs.

| Measurement | Cardiac (%) | Liver (%) | Spleen (%) | Lung (%) | Kidney (%) |
|-----------------------|-------------|---------------------------|--------------------------|-------------|-------------|
| Control (Z) | 0.47 ± 0.03 | 3.15 ± 0.18 ^a | 0.23 ± 0.03 ^b | 0.79 ± 0.23 | 1.21 ± 0.07 |
| Low calcium (D) | 0.47 ± 0.01 | 3.19 ± 0.12 ^a | 0.29 ± 0.01 ^a | 0.66 ± 0.06 | 1.21 ± 0.02 |
| CaCl ₂ (C) | 0.48 ± 0.02 | 2.72 ± 0.46 ^{ab} | 0.30 ± 0.04 ^a | 0.62 ± 0.05 | 1.22 ± 0.06 |
| SBP-Ca (T) | 0.47 ± 0.02 | 2.54 ± 0.26 ^b | 0.23 ± 0.01 ^b | 0.69 ± 0.16 | 1.18 ± 0.16 |

Z: rats fed with AIN-93 diet; D: rats fed with a low calcium AIN-93 diet; C: rats fed with a low calcium AIN-93 diet and CaCl₂; T: rats fed with a low calcium AIN-93 diet and SBP-Ca. The values in columns with different superscript letters are significantly different ($P < 0.05$).

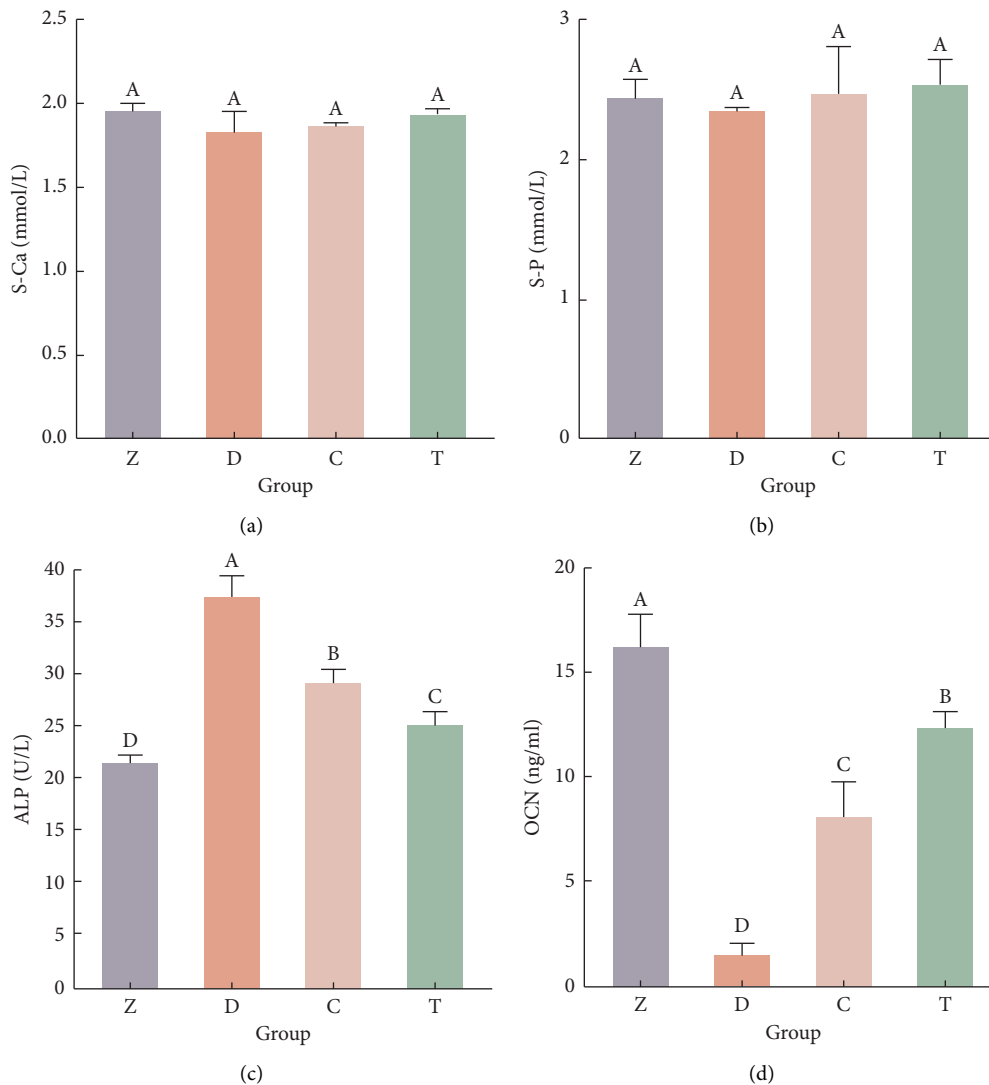


FIGURE 6: Serum calcium (S-Ca; (a)), serum phosphate (S-P; (b)), serum alkaline phosphatase (ALP; (c)), and osteocalcin (OCN; (d)) in rats fed with AIN-93 diet; control group (Z), low calcium AIN-93 diet (D), low calcium AIN-93 diet and CaCl₂ (C), and low calcium AIN-93 diet and SBP-Ca (T).

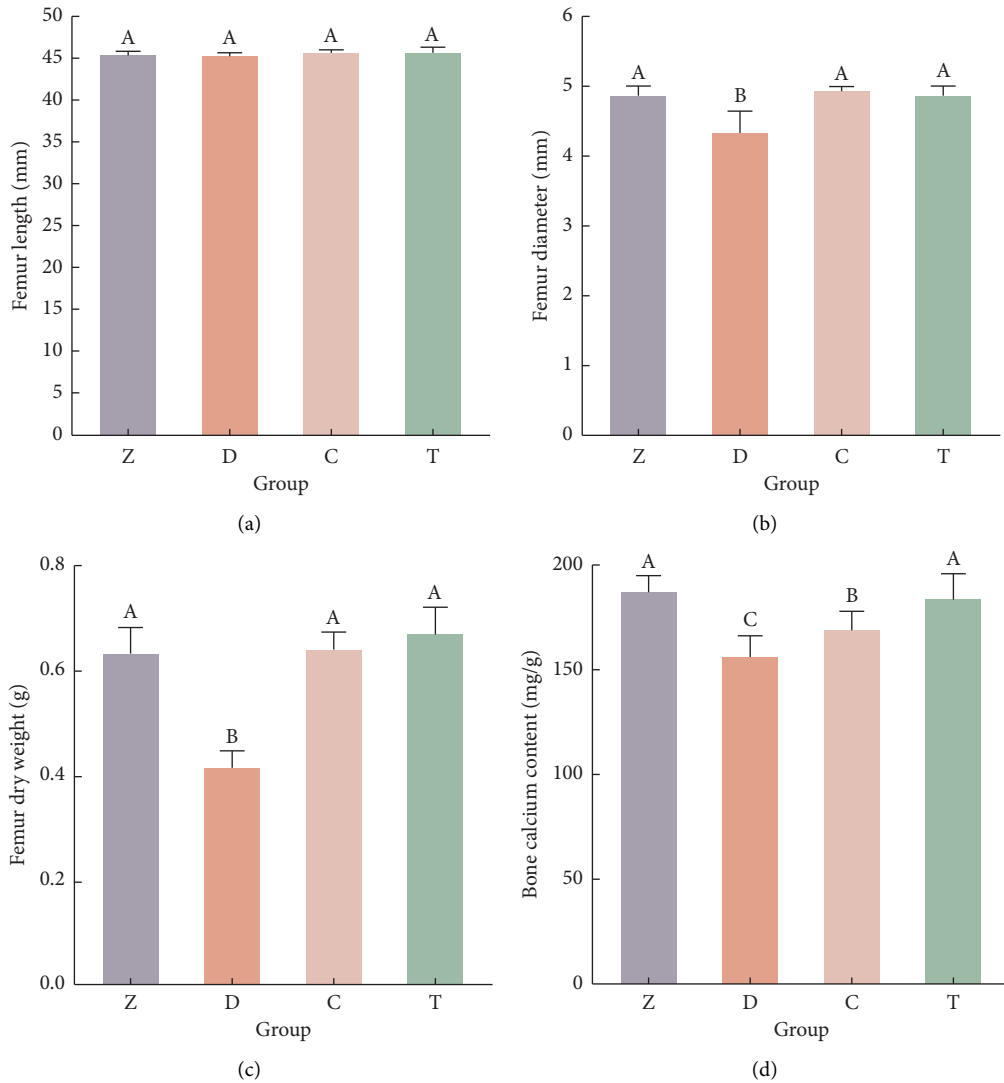


FIGURE 7: Femoral length (a), diameter (b), dry weight (c), and bone calcium content (d) of rats fed with AIN-93 diet; control group (Z), low calcium AIN-93 diet (D), low calcium AIN-93 diet and CaCl₂ (C), and low calcium AIN-93 diet and SBP-Ca (T). Values with different letters differ significantly ($P < 0.05$).

among the groups ($P > 0.05$). Calcium is vital for maintaining body growth and metabolism, so a deficient intake of calcium could have reduced the weight growth rate of the animals [14].

The visceral index is a common evaluation index in toxicological tests, which increases or decreases to varying degrees when the viscera of the animal changes, such as congestion, edema, hypertrophy, or atrophy of the viscera [47]. There were no statistically significant differences observed in the cardiac, lung, and kidney indices between the groups ($P > 0.05$; Table 2). The liver index in group D exhibited a higher value compared to the normal group and the other groups, but the disparity was not statistically significant ($P > 0.05$). A high liver index may be related to liver disorders [48]. These results suggest that SBP-Ca supplementation had no impact on the normal growth and health of rats.

3.7. Effect of SBP-Ca on Serum Biochemical Markers. Compared with group D, the serum calcium and phosphorus levels in groups C and T exhibited elevated serum calcium and phosphorus levels, yet the variance was not statistically significant ($P > 0.05$; Figures 6(a) and 6(b)). This may be due to the dynamic equilibrium between bone calcium and serum calcium. In the case of low daily calcium intake levels, bone calcium will be released into the blood to sustain serum calcium and serum phosphorus concentration at a normal level [49]. ALP and OCN serve as biomarkers for bone formation, providing reliable indicators of osteoblast activity and the status of bone formation. Robison and Soames [50] revealed that ALP was crucial in the upregulation of bone calcification, and its expression increases abnormal calcification. The highest ALP was found in group D ($P < 0.05$; Figure 6(c)), indicating that the rats in this

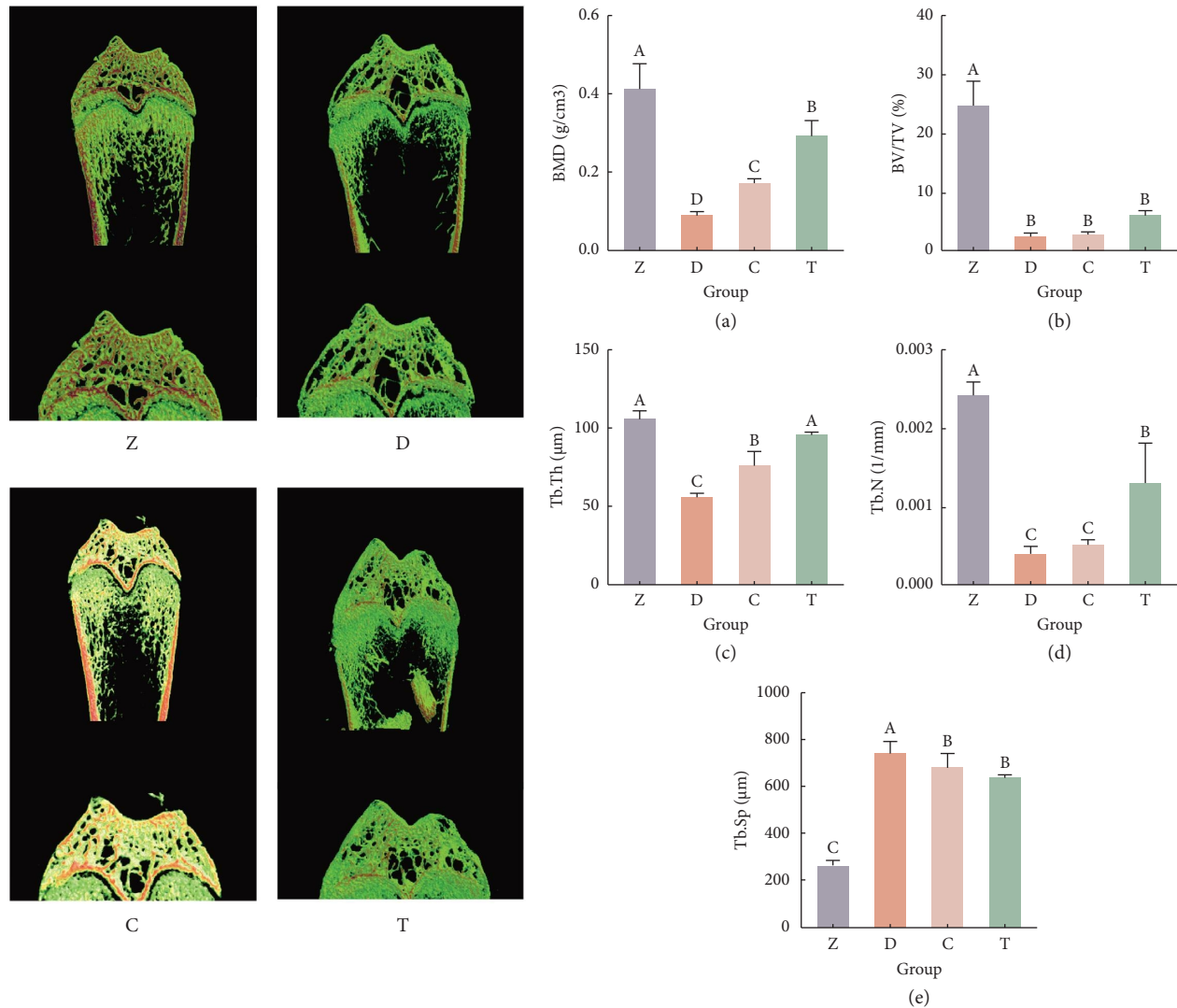


FIGURE 8: Morphological indices of bone mineral density (BMD), bone volume fraction (BV/TV), trabecular thickness (Tb.Th), trabecular number (Tb.N), and trabecular spacing (Tb.Sp) (a–e) of rats fed with AIN-93 diet; control group (Z), low calcium AIN-93 diet (D), low calcium AIN-93 diet and CaCl₂ (C), low calcium AIN-93 diet, and sheep bone peptide-chelated calcium (SBP-Ca) (T). Different letters indicate significant differences ($P < 0.05$).

group were severely calcium deficient and in a state of high bone turnover. This also suggests that a low-calcium diet rat model was successfully established. When supplemented with CaCl₂ and SBP-Ca, ALP activity was significantly reduced ($P < 0.05$). This indicates a negative correlation was identified between ALP activities and Ca intake. These findings align with the observations made by Zhao et al. [51] and others, investigating the impact of desalted duck egg white peptides on calcium absorption in rats and found that serum ALP activity levels could be increased during a long-term low calcium intake. In addition, ALP activity decreased significantly ($P < 0.05$) in the SBP-Ca group (25.17 ± 1.19 U/L) compared to the CaCl₂ group (29.38 ± 1.15 U/L). These results were consistent with the findings reported by Chen et al. [9]. The levels of OCN in group D were notably significantly reduced compared to

the other groups ($P < 0.05$; Figure 6(d)). In group T, the OCN content was significantly ($P < 0.05$) higher (12.43 ± 0.69 ng/mL) than in group C (8.01 ± 1.82 ng/mL). These results further confirm that SBP-Ca supplementation promotes new bone formation and is absorbed more easily in rats [49], which is superior to CaCl₂ supplementation.

3.8. Biochemical Parameters of the Femur. The assimilation and metabolism of calcium may induce alterations in femoral characteristics, so femoral characteristics are ideal monitoring indicators to evaluate the effect of calcium supplementation [52]. There were no notable variations in femur length among the groups ($P > 0.05$; Figure 7(a)). Hernández-Becerra et al. [53] also highlighted that the femur length remained unaffected by the dietary calcium

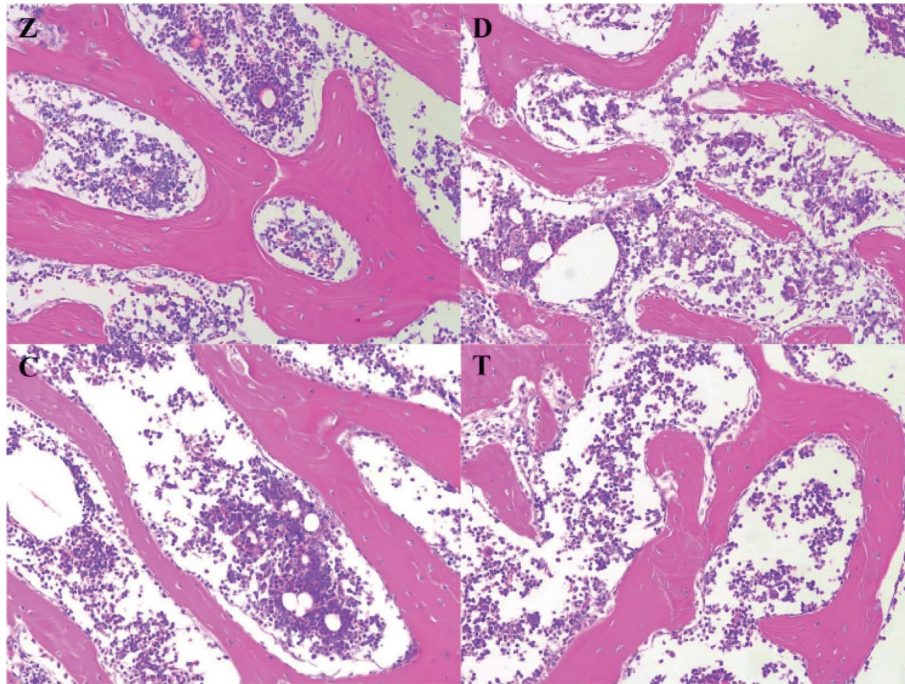


FIGURE 9: H&E staining of femoral transverse section of rats ($\times 20$ magnification); Z: rats fed with AIN-93 diet, control group; D: rats fed with a low calcium AIN-93 diet; C: rats fed with a low calcium AIN-93 diet and CaCl_2 ; T: rats fed with a low calcium AIN-93 diet and SBP-Ca.

deficiency. The diameter and dry weight of the femur of rats in group T exhibited a significantly increase compared to those of group D ($P < 0.05$; Figures 7(b) and 7(c)). This is consistent with the results of Hua et al. [54] who investigated the impact of *Chlorella pyrenoidosa* protein hydrolysate-calcium chelate (CPPH-Ca) on calcium absorption of low-calcium diet-fed rats and found that high doses of CPPH-Ca enhanced the femur and tibial weight index, length, and diameter in rats. Group D (158.09 ± 10.11 mg/g) had a significantly lower femoral calcium content than group Z (191.27 ± 6.15 mg/g; $P < 0.05$; Figure 7(d)). In particular, compared with group D, the bone calcium content increased after dietary supplementation with SBP-Ca and CaCl_2 . Moreover, the bone calcium content within the SBP-Ca-fed group exhibited a notable superiority over that of the CaCl_2 -fed group ($P < 0.05$). From this point of view, the effect of dietary supplementation with SBP-Ca is higher than that of CaCl_2 . These results indicate that SBP-Ca supplementation has a positive effect on calcium absorption, favors the growth and development of rat bones, and can effectively alleviate bone calcium loss. In a similar low-calcium model experiment, Zhao et al. [3] observed a similar phenomenon in the phosvitin phosphopeptide-Ca complex-enhanced calcium absorption and deposition in the rat femur.

3.9. Morphological Analysis of Bone Tissue. Micro-CT has been extensively employed to investigate the alterations in the microstructure of femoral trabeculae in experimental subjects [55]. As shown in Figure 8, group Z had a tight trabecular structure with good continuity, while group D had a severely disrupted trabecular structure with obvious large areas of trabecular-free bone. The bone microstructure

of rats supplemented with SBP-Ca showed more bone trabeculae, fewer areas of boneless trabecular bone, and more intact trabecular junction structures compared to group D. These findings align with the substantial enhancement in bone microstructure and increased trabecular integrity reported by Hua et al. [54] using phosvitin phosphopeptide-Ca in low-calcium diets.

The relevant bone microstructural parameters verified this result, as depicted in Figure 8, compared with group Z; group D exhibited a significantly reduced BMD of the femoral bone, BV/TV, Tb.Th, and Tb.N ($P < 0.05$). Furthermore, the Tb.Sp in the bones of rats was highest in group D ($P < 0.05$), suggesting that the induction of the low-calcium diet rat model was successful. The BMD of rats fed SBP-Ca and CaCl_2 were 0.29 and 0.17 g/cm³, respectively. This indicated that SBP-Ca is more effective than CaCl_2 in bone remineralization. Compared with group D, SBP-Ca supplementation significantly improved femoral Tb.Th and Tb.N and reduced Tb.Sp ($P < 0.05$). These results suggest that SBP-Ca supplementation improves BMD, increases bone mass, preserves bone microarchitecture, and has the potential to ameliorate osteoporosis in rats. A prior investigation suggested that the *Dunaliella salina*-derived peptide could enhance the BMD and trabecular number and decrease trabecular bone space in ovariectomy (OVX) rats [56]; this is similar to our findings.

Furthermore, the histomorphological changes of the transverse section of the femur were examined using H&E staining and observed through an electron microscope [32]. The results of the H&E staining depicting the trabecular structure of the femur are illustrated in Figure 9. The trabecular of the structure bone of the femur in group Z was closely and evenly arranged, and continuity was well-maintained. The

trabecular structure of group D showed dissolution and fractures. In group T, the restoration of trabecular bone quantity in the femur, resulting in increased trabecular bone thickness and reduced intertrabecular space compared to group D. These results indicated that SBP-Ca supplementation significantly increased BMD, improved bone micro-architecture, and enhanced the integrity of bone trabeculae in rats with a low-calcium diet, with a more pronounced effect compared to the use of inorganic calcium (group C).

4. Conclusions

In this study, defatted sheep bone powder was used as the raw material to prepare SBP by double enzymatic hydrolysis. The optimal chelation process of sheep bone peptides with calcium ions (pH = 7, temperature = 45°C, SBP/CaCl₂ mass ratio = 1:1, and time = 60 min) was used to prepare sheep bone peptide-chelated calcium (SBP-Ca). Under these process conditions, the chelation rate of calcium in the SBP-Ca chelate can reach 89.24%. Structural characterization analysis revealed that SBP-Ca is a novel compound distinct from SBP. The carboxyl oxygen atoms, amino nitrogen atoms, and oxygen atoms on the peptide bond in SBP were identified to participate in the chelation of SBP with calcium ions. In addition, the surface of SBP-Ca exhibited a densified structure. Using a rat model, the addition of SBP-Ca in low-calcium diets could promote calcium absorption and increase bone growth and density. Histomorphological studies of bone showed that SBP-Ca could restore the structure of trabecular bone. These results indicate that SBP-Ca supplementation is effective in preventing calcium deficiency and enhancing the bioavailability of calcium. Furthermore, SBP-Ca is more effective than CaCl₂ supplementation in promoting bone formation in rats with low-calcium levels with no side effects detected during the trial. Therefore, SBP-Ca can be used as a novel calcium absorption promoter and may find valuable applications in the prevention of calcium deficiency. However, this study has some limitations, including a relatively short experimental period, a small sample size, and insufficient research depth. Therefore, in the next step, we will expand the sample size and extend the experimental period to 8–12 weeks. We will further explore the mechanism of the ameliorative effect of SBP-Ca on osteoporosis from the following three aspects: intestinal genes, skeletal genes and intestinal flora.

Data Availability

The data used to support the findings of this study are available from the corresponding author upon reasonable request.

Conflicts of Interest

The authors declare that they have no conflicts of interest.

Authors' Contributions

Guanhua Hu and Xiaotong Li contributed equally to this work (cofirst-authors) and performed conceptualization,

data curation, formal analysis, and original draft preparation. Rina Su contributed to conceptualization and data curation. Mirco Corazzin contributed to software and methodology. Lina Sun contributed to investigation and methodology. Lu Dou contributed to conceptualization and data curation. Puxin Hou contributed to investigation and resources. Lin Su contributed to funding acquisition and resources. Ye Jin contributed to supervision, funding acquisition, and reviewing and editing. Lihua Zhao contributed to funding acquisition, investigation, and resources. Ye Jin and Lihua Zhao are cocorresponding authors. Guanhua Hu and Xiaotong Li are the first co-authors.

Acknowledgments

This work was supported by Major Projects of National Agricultural High-Tech Industry Demonstration Zone (Bayan Nur) (NMKJXM202210), Major R&D and Achievements Transformation Projects of Inner Mongolia (2022YFXZ0017), Mechanism of Biogenic Amines-Degrading Ability of *Pediococcus Pentosaceus* 37X-9 Based on LuxS/AI-2 Quorum Sensing System (2023MS03010), and Ministry of Agriculture and Rural Affairs Fresh Beef and Lamb Meat Processing Technology Integration Research Base Capacity Building Project (BR221028).

References

- [1] W. Daengprok, W. Garnjanagoonchorn, O. Naivikul, P. Pornsinpatip, K. Issigonis, and Y. Mine, "Chicken eggshell matrix proteins enhance calcium transport in the human intestinal epithelial cells, Caco-2," *Journal of Agricultural and Food Chemistry*, vol. 51, no. 20, pp. 6056–6061, 2003.
- [2] E. Cho, S. A. Smith-Warner, D. Spiegelman et al., "Dairy foods, calcium, and colorectal cancer: a pooled analysis of 10 cohort studies," *JNCI Journal of the National Cancer Institute*, vol. 96, no. 13, pp. 1015–1022, 2004.
- [3] M. Zhao, D. U. Ahn, S. Li, W. Liu, S. Yi, and X. Huang, "Effects of phosvitin phosphopeptide-Ca complex prepared by efficient enzymatic hydrolysis on calcium absorption and bone deposition of mice," *Food Science and Human Wellness*, vol. 11, no. 6, pp. 1631–1640, 2022.
- [4] A. Afshin, P. J. Sur, K. A. Fay et al., "Health effects of dietary risks in 195 countries, 1990–2017: a systematic analysis for the Global Burden of Disease Study 2017," *The Lancet*, vol. 393, no. 10184, pp. 1958–1972, 2019.
- [5] G. Cormick and J. M. Belizán, "Calcium intake and health," *Nutrients*, vol. 11, no. 7, p. 1606, 2019.
- [6] G. Singh and K. Muthukumarappan, "Influence of calcium fortification on sensory, physical and rheological characteristics of fruit yogurt," *LWT-Food Science & Technology*, vol. 41, no. 7, pp. 1145–1152, 2008.
- [7] L. Guo, P. A. Harnedy, B. Li et al., "Food protein-derived chelating peptides: biofunctional ingredients for dietary mineral bioavailability enhancement," *Trends in Food Science & Technology*, vol. 37, no. 2, pp. 92–105, 2014.
- [8] C. Xixi, Z. Lina, W. Shaoyun, and R. Pingfan, "Fabrication and characterization of the nano-composite of whey protein hydrolysate chelated with calcium," *Food & Function*, vol. 6, no. 3, pp. 816–823, 2015.
- [9] J. Chen, X. Qiu, G. Hao, M. Zhang, and W. Weng, "Preparation and bioavailability of calcium-chelating peptide

- complex from tilapia skin hydrolysates,” *Journal of the Science of Food and Agriculture*, vol. 97, no. 14, pp. 4898–4903, 2017.
- [10] W. Wu, B. Li, H. Hou, H. Zhang, and X. Zhao, “Isolation and identification of calcium-chelating peptides from Pacific cod skin gelatin and their binding properties with calcium,” *Food & Function*, vol. 8, no. 12, pp. 4441–4448, 2017.
- [11] X. L. Bao, Y. Lv, B. C. Yang, C. G. Ren, and S. T. Guo, “A study of the soluble complexes formed during calcium binding by soybean protein hydrolysates,” *Journal of Food Science*, vol. 73, no. 3, pp. C117–C121, 2008.
- [12] Y. Lv, H. Liu, J. Ren, X. Li, and S. Guo, “The positive effect of soybean protein hydrolysates—calcium complexes on bone mass of rapidly growing rats,” *Food & Function*, vol. 4, no. 8, pp. 1245–1251, 2013.
- [13] W. Wu, L. He, Y. Liang et al., “Preparation process optimization of pig bone collagen peptide-calcium chelate using response surface methodology and its structural characterization and stability analysis,” *Food Chemistry*, vol. 284, pp. 80–89, 2019.
- [14] X. Wang, Z. Zhang, H. Xu, X. Li, and X. Hao, “Preparation of sheep bone collagen peptide-calcium chelate using enzymolysis-fermentation methodology and its structural characterization and stability analysis,” *RSC Advances*, vol. 10, no. 20, pp. 11624–11633, 2020.
- [15] J. Dai, L. Tao, Y. Zhou, C. Zhao, J. Sheng, and Y. Tian, “Chelation of walnut protein peptide with calcium and calcium absorption promotion in vivo,” in *IOP Conference Series: Earth and Environmental Science*, IOP Publishing, Bristol, UK, 2020.
- [16] A. Fisher and D. Naughton, “Metal ion chelating peptides with superoxide dismutase activity,” *Biomedicine & Pharmacotherapy*, vol. 59, no. 4, pp. 158–162, 2005.
- [17] H. Guo, Z. Hong, and R. Yi, “Core-shell collagen peptide chelated calcium/calcium alginate nanoparticles from fish scales for calcium supplementation,” *Journal of Food Science*, vol. 80, no. 7, pp. N1595–N1601, 2015.
- [18] W.-K. Jung, B.-J. Lee, and S.-K. Kim, “Fish-bone peptide increases calcium solubility and bioavailability in ovariectomised rats,” *British Journal of Nutrition*, vol. 95, no. 1, pp. 124–128, 2006.
- [19] D. K. Vijayan, P. Sreerexha, P. K. Dara et al., “Antioxidant defense of fish collagen peptides attenuates oxidative stress in gastric mucosa of experimentally ulcer-induced rats,” *Cell Stress & Chaperones*, vol. 27, pp. 45–54, 2022.
- [20] S. Lu, S. Kong, Y. Wang, Z. Hu, L. Zhang, and M. Liao, “Gastric acid-response chitosan/alginate/tilapia collagen peptide composite hydrogel: protection effects on alcohol-induced gastric mucosal injury,” *Carbohydrate Polymers*, vol. 277, Article ID 118816, 2022.
- [21] L. Wang, Y. Zhang, Z. Zhu, F. Zheng, and R. Gao, “Food-derived collagen peptides: safety, metabolism, and anti-skin-aging effects,” *Current Opinion in Food Science*, vol. 51, Article ID 101012, 2023.
- [22] Y. Zhuang, L. Sun, Y. Zhang, and G. Liu, “Antihypertensive effect of long-term oral administration of jellyfish (*Rhopilema esculentum*) collagen peptides on renovascular hypertension,” *Marine Drugs*, vol. 10, no. 12, pp. 417–426, 2012.
- [23] D. König, S. Oesser, S. Scharla, D. Zdzieblik, and A. Gollhofer, “Specific collagen peptides improve bone mineral density and bone markers in postmenopausal women—a randomized controlled study,” *Nutrients*, vol. 10, no. 1, p. 97, 2018.
- [24] E. Porfírio and G. B. Fanaro, “Collagen supplementation as a complementary therapy for the prevention and treatment of osteoporosis and osteoarthritis: a systematic review,” *Revista Brasileira de Geriatria e Gerontologia*, vol. 19, no. 1, pp. 153–164, 2016.
- [25] J. Niu, R. Shao, M. Liu et al., “Porous carbons derived from collagen-enriched biomass: tailored design, synthesis, and application in electrochemical energy storage and conversion,” *Advanced Functional Materials*, vol. 29, no. 46, Article ID 1905095, 2019.
- [26] P. Zhan, H. Tian, X. Zhang, and L. Wang, “Contribution to aroma characteristics of mutton process flavor from the enzymatic hydrolysate of sheep bone protein assessed by descriptive sensory analysis and gas chromatography olfactometry,” *Journal of Chromatography B*, vol. 921–922, pp. 1–8, 2013.
- [27] A. P. Shirsath and M. M. Henchion, “Bovine and ovine meat co-products valorisation opportunities: a systematic literature review,” *Trends in Food Science & Technology*, vol. 118, pp. 57–70, 2021.
- [28] G. Hu, D. Wang, L. Sun et al., “Isolation, purification and structure identification of a Calcium-binding peptide from sheep bone protein hydrolysate,” *Foods*, vol. 11, no. 17, p. 2655, 2022.
- [29] S. El Hajj, R. Irankunda, J. A. Camaño Echavarría et al., “Metal-chelating activity of soy and pea protein hydrolysates obtained after different enzymatic treatments from protein isolates,” *Food Chemistry*, vol. 405, Article ID 134788, 2023.
- [30] P. G. Reeves, F. H. Nielsen, and G. C. Fahey, “AIN-93 purified diets for laboratory rodents: final report of the American Institute of Nutrition ad hoc writing committee on the reformulation of the AIN-76A rodent diet,” *The Journal of Nutrition*, vol. 123, no. 11, pp. 1939–1951, 1993.
- [31] Z. Peng, H. Hou, K. Zhang, and B. Li, “Effect of calcium-binding peptide from Pacific cod (*Gadus macrocephalus*) bone on calcium bioavailability in rats,” *Food Chemistry*, vol. 221, pp. 373–378, 2017.
- [32] B. Liu, L. Sun, and Y. Zhuang, “Protective effects of tilapia (*Oreochromis niloticus*) skin gelatin hydrolysates on osteoporosis rats induced by retinoic acid,” *Food Science and Human Wellness*, vol. 11, no. 6, pp. 1500–1507, 2022.
- [33] Q. Tian, Y. Fan, L. Hao et al., “A comprehensive review of calcium and ferrous ions chelating peptides: preparation, structure and transport pathways,” *Critical Reviews in Food Science and Nutrition*, vol. 63, no. 20, pp. 4418–4430, 2023.
- [34] Z. Bao, P. Zhang, N. Sun, and S. Lin, “Elucidating the calcium-binding site, absorption activities, and thermal stability of egg white peptide-calcium chelate,” *Foods*, vol. 10, no. 11, p. 2565, 2021.
- [35] W. Zhai, D. Lin, R. Mo et al., “Process optimization, structural characterization, and calcium release rate evaluation of mung bean peptides-calcium chelate,” *Foods*, vol. 12, no. 5, p. 1058, 2023.
- [36] S. Fang, G. Ruan, J. Hao, J. M. Regenstein, and F. Wang, “Characterization and antioxidant properties of Manchurian walnut meal hydrolysates after calcium chelation,” *Lwt*, vol. 130, Article ID 109632, 2020.
- [37] X.-M. Xun, Z.-A. Zhang, Z.-X. Yuan et al., “A novel low molecule peptides-calcium chelate from silkworm pupae protein hydrolysate: preparation, antioxidant activity, and bioavailability,” *Current Pharmaceutical Design*, vol. 29, no. 9, pp. 675–685, 2023.
- [38] P. Cui, N. Sun, P. Jiang, D. Wang, and S. Lin, “Optimised condition for preparing sea cucumber ovum hydrolysate-calcium complex and its structural analysis,” *International Journal of Food Science and Technology*, vol. 52, no. 8, pp. 1914–1922, 2017.

- [39] J. Luo, X. Yao, O. P. Soladoye, Y. Zhang, and Y. Fu, "Phosphorylation modification of collagen peptides from fish bone enhances their calcium-chelating and antioxidant activity," *Lwt*, vol. 155, Article ID 112978, 2022.
- [40] A. Barth, "The infrared absorption of amino acid side chains," *Progress in Biophysics and Molecular Biology*, vol. 74, no. 3-5, pp. 141-173, 2000.
- [41] M. Nara and M. Tanokura, "Infrared spectroscopic study of the metal-coordination structures of calcium-binding proteins," *Biochemical and Biophysical Research Communications*, vol. 369, no. 1, pp. 225-239, 2008.
- [42] J. Wang, B. Zhang, W. Lu et al., "Cell proliferation stimulation ability and osteogenic activity of low molecular weight peptides derived from bovine gelatin hydrolysates," *Journal of Agricultural and Food Chemistry*, vol. 68, no. 29, pp. 7630-7640, 2020.
- [43] D. Blat, L. Weiner, M. B. Youdim, and M. Fridkin, "A novel iron-chelating derivative of the neuroprotective peptide NAPVSIPQ shows superior antioxidant and anti-neurodegenerative capabilities," *Journal of Medicinal Chemistry*, vol. 51, no. 1, pp. 126-134, 2008.
- [44] A. Armas, V. Sonois, E. Mothes, H. Mazarguil, and P. Faller, "Zinc (II) binds to the neuroprotective peptide humanin," *Journal of Inorganic Biochemistry*, vol. 100, no. 10, pp. 1672-1678, 2006.
- [45] R. P. Houser, M. P. Fitzsimons, and J. K. Barton, "Metal-dependent intramolecular chiral induction: the Zn²⁺ complex of an ethidium-peptide conjugate," *Inorganic Chemistry*, vol. 38, no. 6, pp. 1368-1370, 1999.
- [46] X. Wang, A. Gao, Y. Chen, X. Zhang, S. Li, and Y. Chen, "Preparation of cucumber seed peptide-calcium chelate by liquid state fermentation and its characterization," *Food Chemistry*, vol. 229, pp. 487-494, 2017.
- [47] X. Qin, Q. Shen, Y. Guo et al., "Physicochemical properties, digestibility and anti-osteoporosis effect of yak bone powder with different particle sizes," *Food Research International*, vol. 145, Article ID 110401, 2021.
- [48] M. S. Islam, H. Yu, L. Miao, Z. Liu, Y. He, and H. Sun, "Hepatoprotective effect of the ethanol extract of *Illicium henryi* against acute liver injury in mice induced by lipopolysaccharide," *Antioxidants*, vol. 8, no. 10, p. 446, 2019.
- [49] D. Chen, X. Mu, H. Huang, R. Nie, Z. Liu, and M. Zeng, "Isolation of a calcium-binding peptide from tilapia scale protein hydrolysate and its calcium bioavailability in rats," *Journal of Functional Foods*, vol. 6, pp. 575-584, 2014.
- [50] R. Robison and K. M. Soames, "The possible significance of hexosephosphoric esters in ossification: Part II. The phosphoric esterase of ossifying cartilage," *Biochemical Journal*, vol. 18, no. 3-4, pp. 740-754, 1924.
- [51] N. Zhao, J. Hu, T. Hou, Z. Ma, C. Wang, and H. He, "Effects of desalted duck egg white peptides and their products on calcium absorption in rats," *Journal of Functional Foods*, vol. 8, pp. 234-242, 2014.
- [52] T. Applegate and M. Lilburn, "Growth of the femur and tibia of a commercial broiler line," *Poultry Science*, vol. 81, no. 9, pp. 1289-1294, 2002.
- [53] E. Hernández-Becerra, D. Jiménez-Mendoza, N. Mutis-Gonzalez, P. Pineda-Gomez, I. Rojas-Molina, and M. E. Rodríguez-García, "Calcium deficiency in diet decreases the magnesium content in bone and affects femur physicochemical properties in growing rats," *Biological Trace Element Research*, vol. 197, no. 1, pp. 224-232, 2020.
- [54] P. Hua, Y. Xiong, Z. Yu, B. Liu, and L. Zhao, "Effect of *Chlorella pyrenoidosa* protein hydrolysate-calcium chelate on calcium absorption metabolism and gut microbiota composition in low-calcium diet-fed rats," *Marine Drugs*, vol. 17, no. 6, p. 348, 2019.
- [55] I. Y. Kim, S. S. Yi, J. H. Shin et al., "Intensive morphometric analysis of enormous alterations in skeletal bone system with micro-CT for AHNAK^{-/-} mice," *Anatomical Science International*, vol. 95, no. 3, pp. 323-333, 2020.
- [56] Y. Chen, J. Chen, Y. Zheng et al., "Dunaliella salina-derived peptide protects from bone loss: isolation, purification and identification," *Lebensmittel-Wissenschaft und-Technologie*, vol. 137, Article ID 110437, 2021.